

Strain hardening and softening in nanotwinned Cu

Rongmei Niu and Ke Han*

National High Magnetic Field Laboratory/Florida State University, 1800 E Paul Dirac Dr., Tallahassee, FL 32310, USA

Received 25 January 2013; revised 21 February 2013; accepted 23 February 2013

Available online 6 March 2013

Nanotwinned Cu foils with about 99% coherent twin boundaries (TBs) among all the boundaries were made. These coherent TBs, with an average spacing of 25 nm, were engineered approximately parallel to foil surfaces. Low plane-strain deformation enhances the hardness by refining microstructure and introducing dislocations. High plane-strain deformation results in crystallographic lattice rotation and reaction between dislocations and coherent TBs, and induces incoherent TBs, thus twin coarsening and even diminishing of nanotwins accompanied by recovery and recrystallization, which cause softening.

© 2013 Acta Materialia Inc. Published by Elsevier Ltd. All rights reserved.

Keywords: Nanostructured materials; Twinning; Coarsening; Softening; Recovery

Materials such as Cu-containing nanoscale growth twins have been reported to have an attractive combination of properties, including high strength [1–7], ductility and stability [7–10]. Given the unusual properties obtained in nanotwinned (NT) materials, they can be exploited in a variety of structural and functional applications, and have been a subject of research for years. Many advances have been made in processing techniques, improving mechanical properties and relating the microstructure to mechanical properties in NT materials. Various microstructural features, such as grain morphology, orientation of twin boundaries (TBs) [11,12] and texture, influence the strength of NT samples, while the strength is mainly governed by twin spacing [4–6,13,14]. For instance, it was reported that, when the average twin spacing in {111}-textured Cu shrank from 100 to 5 nm, the strength was increased from about 0.3 to 1.1 GPa [4,5,14]; in {110}-textured Cu [15], the strength reached 0.9 GPa with reduction of the twin spacing to 15 nm [2,16]. Moreover, the microstructure can be refined by cold deformation, and the refinement is proportional to the macrostrain; this is another method to enhance the mechanical strength [17]. Room temperature (RT) strain hardening has indeed been reported in rolled (110)-textured NT Cu [15]. However, grain or twin growth in nanocrystalline metals under deformation has also been reported, and softening was observed in nanocrystalline Cu left

for extended periods of time at RT [9,18–24]. It is unclear whether the deformation-enhanced hardness in NT Cu can be maintained during long-term service, though the stability of nanotwin boundaries in copper under different mechanical loading states has been heavily investigated [9,10,25]. If a TB is stable, it is important to find the critical deformation strain to achieve the possible highest strength, because softening was reported in NT Cu with a twin spacing of less than 15 nm [2,20]. As a consequence, the characterization of deformation-related stability in NT Cu is studied in this work.

High-purity Cu foils ($50 \times 10 \times 0.1\text{--}0.2 \text{ mm}^3$ in size) were synthesized by a pulsed electro-deposition technique. The details of the preparation are described in Ref. [21]. Some of the as-deposited foils were cold deformed in a plane-strain condition by rolling with the rolling plane perpendicular to the growth direction of foils.

Microhardness tests were performed on a Tukon 2100 microhardness tester with a Vickers diamond pyramid indenter on both the substrate sides and cross-sections of as-deposited, rolled and aged foils, complying with the procedure in ASTM E384. The hardness of the rolled samples was measured immediately after rolling. To select the most suitable load, hardness was measured with loads of 50, 100 and 300 g on typical samples, and the corresponding hardness numbers were found to be within a 3% range. The indents were larger than 20 μm in the diagonal [24]. Further indents examinations revealed that the indent depths were only 2, 3 and 5.5 μm , respectively. Therefore, the foil thickness was at least 10 times the depth of indentation [22,23].

* Corresponding author. Tel.: +1 850 644 6746; fax: +1 850 644 0867; e-mail: han@magnet.fsu.edu

No marks could be observed on the opposite surfaces. To confine and minimize the deformation zone within the foil under indentation without losing any accuracy, a 50 g load was selected and used to generate the data reported in this paper. The time duration was 10 s. Our scanning electronic microscopy (SEM) observations at the cross-section of indenters revealed that the visible deformation zone under the indentation tip was less than 1 μm , which further confirmed that 50 g was a proper load for measuring the hardness. This load was considered not so high as to penetrate the foils but not so low as to overestimate/underestimate the mechanical property. Six to ten tests were conducted for each measurement. The microstructures of the as-deposited, rolled and aged Cu were characterized by both SEM and transmission electronic microscopy (TEM; JOEL-2011) on the cross-sections. The cross-section TEM samples were prepared by twin-jet electropolishing. The details are presented in Ref. [26,27].

Figure 1 and Supplementary Figure S1(a) show that the as-deposited Cu has a columnar structure filled with a high density of $\{111\}$ growth twins roughly parallel to the substrate surfaces. The average angle between the TBs and substrate is close to 0.8° . The average twin spacing is measured to be around 25 nm. Two distinct features are shown. First, the coarse columnar (about 4 μm) is two orders of magnitude wider than the twins. Hence it is reasonable to assume that the hardness is primarily determined by the twin spacing, rather than the twin length (columnar size) in our materials. Second, most of the TBs are coherent ($\sim 99\%$) and extend laterally across the entire column, with the densities of incoherent TBs and arbitrary angle GBs being about 1%. The correspondent select area diffraction pattern (SADP; see the inset in Fig. 1) shows that most of the diffraction spots appear to be elongated in the $\langle 111 \rangle$ direction due to the overlapping of the streaks with primary diffraction spots, which confirms the high density of TBs. The coherent TB energies (24 mJ m^{-2}) are an order of magnitude lower than those of conventional GBs (625 mJ m^{-2}) [28]. From the above values, the total coherent TBs and GBs energies are estimated to be 0.96 and 0.416 mJ mm^{-3} , respectively, for our NT Cu.

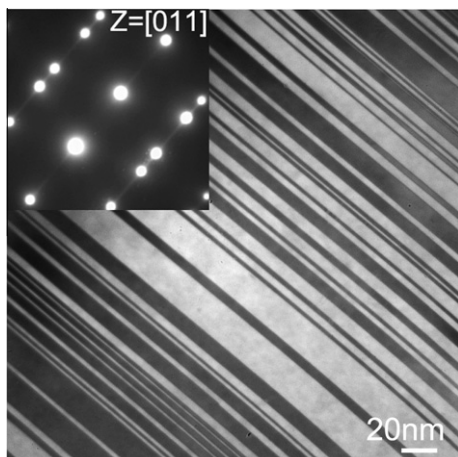


Figure 1. Bright field TEM image showing the high density of coherent TBs in as-deposited NT Cu.

For Cu with a grain size at RT of 100 nm, which is close to the stable grain size at ambience, the grain boundary energy is calculated to be about 18.7 mJ mm^{-3} , which is an order of magnitude larger than the stored TB energy in our materials. The calculated results indicate that as-deposited Cu samples have nearly no driving force for twin coarsening or detwinning (detwinning loosely refers to an irreversible twin coarsening process in this work) at RT without external turbulence. This estimation is further confirmed by our experimental observations. Heat treatments at 100°C for 72 h or aging at ambience over a year have been respectively conducted on as-deposited Cu. The densely twinned/matrix lamellar structure is found to be stable, and no detectable variation in the twin spacing or orientation of twin boundaries is observed. Our materials with above relatively simple structure were chosen for further rolling experiments.

As illustrated in Figure 2, the trend of the enhancement of hardness on the substrate sides by rolling is consistent with the expected and previous results [15,29] when the true strain is less than 20%. However, when the true strain reaches 40%, work softening takes place. Therefore the critical strain is about 20% for hardening in our system. To determine whether such a softening was time related, aging experiments at ambience were undertaken with the rolled samples. Figure 2 shows that the hardness drops significantly during aging. Since the major deformation strain directions are either parallel or perpendicular to the twin boundaries in our plane-strain condition, it is hypothesized that the density of incoherent TBs cannot remain as negligible as that in the as-deposited Cu. Accordingly, we investigated our samples in an effort to understand the softening mechanism in NT materials as a result of deformation.

Figure 3 illustrates the hardness evolution of rolled NT Cu on substrate sides during isothermal aging at RT. It is seen that the hardness of the rolled Cu achieved at RT begins to decay within a few days. An increase in the cold-rolling strain accelerates the hardness recession. For example, the hardness of the Cu foils at a true strain of 71% drops by 19% in 5 days, in contrast to the slight hardness decrease of 11% at a true strain of 51%. In about 12 days, the hardness values of Cu with a true strain of 15% decrease by only 9%, while the values of Cu at a true strain of 71% drop pronouncedly, by

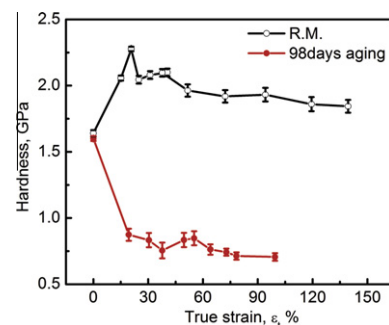


Figure 2. Strain-related age-softening curves of rolled NT Cu. “R.M.” and “98 days aging” mean that hardness measurements are taken immediately after rolling and after 98 days of aging of rolled NT Cu, respectively.

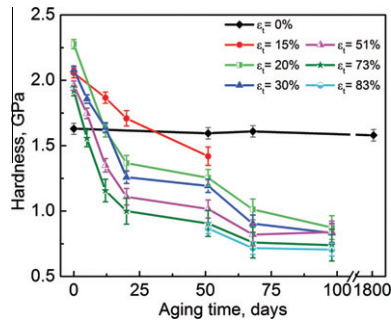


Figure 3. RT hardness vs. aging time in NT Cu at different true strains, $\epsilon_t\%$.

40%. The hardness of the deformed NT Cu continues to fall over a very considerable aging period. By contrast, the hardness of as-deposited Cu foils shows no evident change during long-term aging, showing outstanding stability (Fig. 3). This is consistent with our microstructure observations.

Deformation changes the structure of the nanotwins. The SEM observations in Supplementary Figure S1(b) and (c) show twin spacing before and after deformation, respectively. In the marked area, the twin spacing is shrunk by 13% after a true strain of 20%, which suggests that most of the strain hardening under a small strain can be attributed to the reduction in twin spacing.

Figure 4(a) shows that dislocations are tangled adjacent to or with TBs in rolled Cu at a true strain of 24%. The corresponding SADP demonstrates that the diffraction spots become arched (see e.g. the $\{422\}$ spots), indicating crystal rotation. With an increase in deformation strain to 71%, the fine-twinned lamellar structure is replaced by a coarse lamellar one (Fig. 4(b)). Figure 4(b) also reveals an uneven microstructural response to thermomechanical processing: some laminar grains are significantly widened and coarsened, while others remain very fine. Further rolling deformation shortens the coarsening process and introduces recrystallization. Figures 4(c) and S1(d) show evidence of the formation of a large area of new grains via recrystallization under a true strain of 86% after 1 week of aging, though some fine NTs can still be seen.

With deformation in the rolled NT Cu, TBs rotation and the softening mechanism are schematically modeled in Figure S2(a)–(f). If the twin/matrix lamellar struc-

tures in the as-deposited NT Cu are defined as T1 and T2 crystals that have a twin orientation relationship to each other (Fig. S2(a), all the T1 crystals have the same orientation in the crystallographic space and so do the ones in T2. The sizes of T1 and T2 are almost identical. Rotation can occur within either T1 or T2, or in both of them. For the former case, the arched spots are considered to be due to a formation of low-angle GBs within a single crystal in either T1 or T2 (Fig. S2(b)). The dislocation distance induced by crystal rotation is calculated to be about 4 nm, which suggests that only a few dislocations can exist within a twin with spacing of 25 nm. This calculation is consistent with our current observations in the imaging mode that very few dislocations are found within the grains. However, no arrays of dislocations (i.e. more than 5) observed to form the low-angle GBs are responsible for lattice rotation within 25 nm. Hence, the major rotations should occur among a group of crystals in T1 and T2 (Fig. S2(c)). In other words, the crystals defined as T1 in the as-deposited conditions deviate from the original orientation established in the as-deposited condition, and the twin boundaries are no longer exactly parallel to the twin plane. The rotations among different grains can result in the reaction of tangled dislocations with TBs due to the narrow twin spacing (25 nm). Such reaction leads to the generation of twinning dislocations [28,30–32] and incoherent TBs, and reduces the density of fully and perfectly coherent TBs. The deposited dislocations on TBs may contribute to the strength of NT Cu by increasing the slide resistance of other dislocations that are impinging TBs, provided that the dislocations do not react with the TBs. However, due to the reaction, such dislocations contribute limited strengthen to the materials, since the dislocation migration distance remains almost the same with just the addition of dislocations at TBs. At the same time, an increase in incoherent TBs makes the overall TBs more mobile under stresses because Shockley partial dislocations with increased density can glide on (111) planes. Upon further deformation, more and more TBs lose their coherency and become dislocation sources, and the applied shear stress enables these incoherent boundaries to migrate easily [31], which weakens the barrier to dislocation activity. The loss of coherency is accompanied by recovery because no significant increase in the dislocation densities is observed in our samples even when the deformation strain reaches about

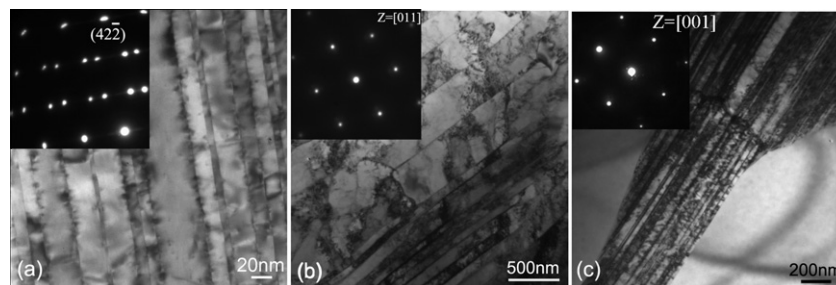


Figure 4. TEM images showing the evolution of the cross-sectional microstructure with rolling deformation conditions. (a) Curved TBs with dislocations lying in TBs in Cu rolled to a true strain of 24% (inset: SADP showing the rotation of the lattice at $g = \{422\}$); (b) the progression of recovery of the deformed samples at a true strain of 71% (inset: SADP exhibiting the disappearance of twins); (c) recrystallization at a true strain of 86% (inset: SADP indicating the formation of new large grains).

40%, and the major activities in the recovery process are the dislocation annihilations. At a later stage, twin coarsening or detwinning is triggered (Fig. S2(d) and (e)), which is caused by the annihilation of coherent TBs and is responsible for the abnormal softening phenomenon in rolled NT Cu at intermediate deformation strains. The higher the rolled strains, the more the stored strain energy drives dislocations to rearrange into lower energy configurations. Eventually, recrystallization occurs (Fig. S2(f)), as exhibited by a dramatic drop in hardness.

The above analyses do not imply that the softening occurs homogeneously. Differences in both orientation [11,12,32] and the magnitude of deformation strain/stress [9,29] may result in variations in a material's response to strain. In our case, the average hardness obtained on the cross-sections is about 0.3 GPa lower than that on the substrate sides. Because deformation is never practically uniform in rolling deformation, recovery, recrystallization and grain growth dominate the microstructure's evolution in some preferred locations, while in others the original twin spacing remains almost intact (Fig. 4(c)).

In summary, NT Cu with a (111) texture is deposited and deformed under plane-strain conditions. Its stability is assessed as a function of deformation strain and aging times. The as-deposited NT Cu is stable. By contrast, softening occurs in the rolled Cu and is accelerated by an increase in deformation strains, i.e. stored strain energy. The stored strain energy is related to dislocations, incoherent TBs/partial dislocations and rotation of the TBs, which are the driving forces for twin coarsening or detwinning, recovery and recrystallization. Studies of this unusual and strain-induced softening will help us to understand how the reliability of NT materials is dependent on coherent TBs.

The authors express their appreciation of Drs. L. Lu and K. Lu for supplying some of the samples used in the early work and Drs. J.R. Weertman and B.Z. Cui for discussions. This research was supported by a UCGP grant in the National High Magnetic Field Laboratory, which is supported by NSF Cooperative Agreement No. DMR-0654118 and DMR 1157490, by the State of Florida, and by the US Department of Energy.

Supplementary data associated with this article can be found, in the online version, at <http://dx.doi.org/10.1016/j.scriptamat.2013.02.051>.

- [1] L. Lu, Y.F. Shen, X.H. Chen, L.H. Qian, K. Lu, *Science* 304 (2004) 422–426.
 [2] L. Lu, X. Chen, X. Huang, K. Lu, *Science* 323 (2009) 607–610.

- [3] K. Han, R.P. Walsh, A. Ishmaku, V. Toplosky, L. Brandao, J.D. Embury, *Philos. Mag.* 84 (2004) 3705–3716.
 [4] X. Zhang, H. Wang, X.H. Chen, L. Lu, K. Lu, R.G. Hoagland, A. Misra, *Appl. Phys. Lett.* 88 (2006) 173116.
 [5] O. Anderoglu, A. Misra, H. Wang, F. Ronning, M.F. Hundley, X. Zhang, *Appl. Phys. Lett.* 93 (2008) 083108.
 [6] K.A. Afanasyev, F. Sansoz, *Nano Lett.* 7 (2007) 2056–2062.
 [7] X. Zhang, A. Misra, H. Wang, J.G. Swadener, A.L. Lima, M.F. Hundley, R.G. Hoagland, *Appl. Phys. Lett.* 87 (2005) 233116.
 [8] O. Anderoglu, A. Misra, H. Wang, X. Zhang, *J. Appl. Phys.* 103 (2008) 094322.
 [9] C.J. Shute, B.D. Myers, S. Xie, T.W. Barbee, A.M. Hodge, J.R. Weertman, *Scr. Mater.* 60 (2009) 1073–1077.
 [10] X. Zhang, A. Misra, *Scr. Mater.* 66 (2012) 860–865.
 [11] J.C. Ye, Y.M. Wang, T.W. Barbee, A.V. Hamza, *Appl. Phys. Lett.* 100 (2012).
 [12] Z. You, X. Li, L. Gui, Q. Lu, T. Zhu, H. Gao, L. Lu, *Acta Mater.* 61 (2013) 217–227.
 [13] L.L. Shaw, A.L. Ortiz, J.C. Villegas, *Scr. Mater.* 58 (2008) 951–957.
 [14] Z.S. You, L. Lu, K. Lu, *Acta Mater.* 59 (2011) 6927–6937.
 [15] Z.S. You, L. Lu, K. Lu, *Scr. Mater.* 62 (2010) 415–418.
 [16] X.H. Chen, L. Lu, K. Lu, *Scr. Mater.* 64 (2011) 311–314.
 [17] J.D. Embury, A.S. Keh, R.M. Fisher, *Trans. Metall. Soc. AIME* 236 (1966) 1252–1259.
 [18] B. Günther, A. Kumpmann, H.D. Kunze, *Scripta Metall. Mater.* 27 (1992) 833–838.
 [19] A.M. Hodge, T.A. Furnish, C.J. Shute, Y. Liao, X. Huang, C.S. Hong, Y.T. Zhu, T.W. Barbee, J.R. Weertman, *Scr. Mater.* 66 (2012) 872–877.
 [20] S.M. Han, M.A. Phillips, W.D. Nix, *Acta Mater.* 57 (2009) 4473–4490.
 [21] B.Z. Cui, K. Han, Y. Xin, D.R. Waryoba, A.L. Mbaruku, *Acta Mater.* 55 (2007) 4429.
 [22] G.F. Vander Voort, G.M. Lucas, *Adv. Mater. Processes* 154 (1998) 21–26.
 [23] A. Stone, D.H. Herring, *Industrial Heating - Pittsburgh Then Troy* 73 (2006) 83–85.
 [24] G.F. Vander Voort, R. Fowler, *Adv. Mater. Processes* 170 (2012) 28–33.
 [25] A.M. Hodge, T.A. Furnish, C.J. Shute, Y. Liao, X. Huang, C.S. Hong, Y.T. Zhu, T.W. Barbee Jr., J.R. Weertman, *Scr. Mater.* 66 (2012) 872–877.
 [26] K. Han, K. Yu-zhang, *Scripta Mater.* 50 (2004) 781–786.
 [27] R.M. Niu, K. Han, *Microsc. Res. Tech.* in press.
 [28] J.P. Hirth, L. Lothe, *Theory of Dislocations*, second ed., John Wiley & Sons, New York, 1982.
 [29] O. Anderoglu, A. Misra, J. Wang, R.G. Hoagland, J.P. Hirth, X. Zhang, *Int. J. Plast.* 26 (2010) 875–886.
 [30] J.W. Christian, S. Mahajan, *Prog. Mater. Sci.* 39 (1995) 1–157.
 [31] X.L. Dongchan Jang, Huajian Gao, Julia R. Greer, *Nat. Nanotechnol.* 7 (2012) 594–601.
 [32] D.C. Jang, X.Y. Li, H.J. Gao, J.R. Greer, *Nat. Nanotechnol.* 7 (2012) 594–601.